ISSN: 3033-3652

Journal of Physical Mathematics & its Applications

SCIENTIFIC Research and Community

Research Article

Open Access

Development of a Physico-Mathematical Model of the Unsteady Combustion Process of a Solid Propellant

Elena Vladimirovna Alves and Manuel Joaquim Alves*

Instituto Superior de Ciencias e Tecnologia de Moçambique (ISCTEM), Mozambique

***Corresponding author**

Manuel J Alves, Instituto Superior de Ciencias e Tecnologia de Moçambique (ISCTEM), Mozambique.

Received: January 26, 2026; **Accepted:** October 26, 2026; **Published:** November 02, 2026

Introduction

The modelling of solid-propellant combustion requires rigorous integration of physics, mathematics, numerical analysis, and experimental evidence. This project preserves that integration from problem definition through to the assessment of predictive capability. Rather than beginning with an isolated expression, the development starts from the essential physical mechanisms and constructs, phase by phase, a verifiable and documented chain consistent with the literature on combustion, propulsion, and moving-boundary problems [1-4].

Phase I identifies the physical system, assumptions, observable quantities, and parameters. Phase II converts this specification into a dimensional system while keeping the kinematics of the regressing surface explicit. Phase III introduces scales and dimensionless groups [5-6]. Phase IV establishes discretisation, coupling, and numerical verification, following the principle that the code must demonstrate that it solves the equations correctly before being used for physical inference [7-12].

Phase V completes the cycle by addressing calibration, experimental validation, sensitivity, and uncertainty quantification [13–16]. Calibration is not validation: calibration estimates parameters from specified data, whereas validation evaluates performance against independent observations within the defined application domain [12-17]. This distinction reduces the risk of confusing goodness of fit with predictive capability.

The project adopts a hierarchy of models. Development begins with a one-dimensional representation using effective properties and controllable mechanisms, with complexity increased only when justified by the data and validation residuals. This strategy favours identifiability and physical interpretation, since additional parameters without sufficient experimental information may increase uncertainty without improving explanatory power [18].

Thermal memory receives particular attention. In an unsteady process, the surface response depends on the temperature field created by the history of heating and regression. Pressure or heat-flux disturbances may therefore produce delays and relaxation phenomena that cannot be described solely by the instantaneous external state. The model seeks to represent this memory through the dynamics of the governing equations themselves.

The phase-based organisation establishes control points: a physical assumption must be traceable to the formulation; a term in an equation must appear in the discretisation; a calibrated parameter must be linked to an information source; and a prediction must be accompanied by a measure of uncertainty. The bibliography is integrated throughout the work to place these decisions within established references [19-22].

The document is therefore intended to serve both as a scientific foundation and as an implementation roadmap. The five phases lead from the initial physical question to quantitative comparison between simulation and experiment, providing a basis for parametric exploration, model extension, and the production of reproducible results.

Overview of Phases I–V

This document brings together, in a single sequence, the first five phases of the project. **Phase I** establishes the physical foundations; **Phase II** constructs the dimensional moving-boundary system; **Phase III** nondimensionalises the problem; **Phase IV** defines the numerical method and computational verification; and **Phase V** establishes calibration, experimental validation, sensitivity analysis, and uncertainty quantification.

Methodological Continuity

Eliminaro título duplicado
Phases I–V form a single chain: physics → formulation → scales → numerical solution → comparison with data. Progression between phases is accepted only when the criteria of the preceding stage have been documented.

PHASE I – Physical Foundations and Specification

Objective of Phase I

The first phase defines the physical problem before the governing equations are written in their definitive form. The objective is to identify the mechanisms essential to the description of unsteady combustion, establish the working assumptions, select the observable quantities, and define a data architecture that will support subsequent calibration and validation [23-27].

The model should explain the thermal response of the propellant, decomposition in the condensed phase, surface regression, and

the influence of external conditions, while preserving the thermal memory generated by the time evolution of the temperature field. This approach avoids introducing a physical counterpart and reduces ambiguity at the formulation stage.

Physical Description of the System

A solid propellant is considered which, at each instant, occupies the region extending inward from the burning surface. The gas phase transfers energy to the interface; part of this energy is conducted into the solid, part participates in interfacial processes, and part may be lost through radiation or other mechanisms included in the experimental configuration.

Heating induces thermal decomposition and changes the state of the material within a layer close to the surface. As the propellant is consumed, the interface moves. Under unsteady conditions, the regression rate does not depend solely on instantaneous conditions: the thermal field accumulated within the solid carries information about the recent history of the system.

Physical core
The problem arises from the coupling of **thermal conduction, decomposition kinetics, surface regression**, **and gas-phase heat feedback**. The moving boundary links these four mechanisms.

Baseline Assumptions

The first version of the model adopts deliberately controlled assumptions: one-dimensional geometry normal to the surface; a condensed medium represented by effective properties; spatially uniform gas pressure on the local scale; conduction as the dominant mechanism of heat transport within the solid; decomposition described by a conversion variable; and a well-defined surface whose position varies with time.

These assumptions are not regarded as universal. They constitute a minimum configuration to which temperature-dependent properties, multiple reactions, radiation, porosity, residual-layer formation, erosive effects, or more detailed coupling with the gas phase may subsequently be added.

Domain, Coordinate, and Interface

Let x denote the coordinate normal to the surface and directed into the propellant. The instantaneous interface position is $x = s(t)$, and the solid occupies $x > s(t)$. The positive regression rate will be defined, at the mathematical stage, consistently with surface recession.

This orientation must remain unchanged throughout the project. Any subsequent change would affect the signs of the conductive heat flux, interface kinematics, and energy balance. The geometrical convention is therefore treated as structural information rather than as a notational detail.

State Variables

The minimum selected variables are temperature $T(x, t)$, degree of conversion $\alpha(x, t)$, surface position $s(t)$, and regression rate $r(t)$. The surface temperature is denoted by $T_s(t) = T(s(t), t)$.

The variable α takes values between zero and one and represents, in an effective description, the progress of the thermal transformation of the material. The position s(t) contains geometrical information about propellant consumption, whereas $r(t)$ quantifies the rate of that consumption.

Thermophysical Parameters

The minimum specification requires solid density ρs, specific heat capacity cs, and thermal conductivity ks. The combination $\kappa s = ks/(\rho scs)$ defines the thermal diffusivity and provides a first scale for estimating the depth of heat penetration.

Where sufficient experimental data are available, ks, cs, and possibly ρs may depend on temperature and degree of conversion. In the absence of robust data, the initial version will employ constant effective values accompanied by sensitivity analysis.

Decomposition Kinetics

Decomposition should be represented by a kinetic law whose complexity is commensurate with the available experimental information [1-19]. As a starting point, an Arrhenius-type form is considered, with pre-exponential factor A, activation energy E_a, effective reaction order n, and universal gas constant Ru.

Adopting a single-step model does not imply that the actual chemical mechanism is elementary. It is an effective representation intended to reproduce the dominant time scale of the transformation. If thermoanalytical tests reveal clearly separated multiple stages, the structure should be extended accordingly.

Surface Regression

Surface regression provides the link between material transformation and domain geometry [3,31]. Under steady conditions, empirical pressure–burning-rate laws may provide a reference. For the unsteady problem, however, the regression law should allow dependence on surface temperature, pressure, and, where necessary, degree of conversion.

The objective is not to impose a unique expression in advance, but to define which variables must enter the closure relation. The final form will be selected on the basis of physical consistency, parameter identifiability, and the ability to reproduce transient experiments.

Gas-Phase Heat Feedback

The gas phase influences the solid primarily through the heat flux returned to the surface. In a first approximation, this flux may be represented by an effective heat-transfer coefficient and a difference between a characteristic gas temperature and the surface temperature.

Where radiation is significant, it should be treated separately. Distinguishing between effective convective heat flux, radiative contribution, and energy consumed at the interface is essential to prevent a single parameter from absorbing physically distinct mechanisms.

Interfacial Energy Balance

The interface must satisfy energy conservation. The heat flux supplied by the gas is partitioned among conduction into the interior, energetic effects associated with transformation and regression, and any losses that may be present. Phase I establishes this architecture; Phase II will write the corresponding dimensional condition with explicit sign conventions.

Consistency rule
No term may be added to the interfacial balance without specifying its physical origin, unit, sign, associated parameter, and the experimental or bibliographical basis used to determine it.

Initial Conditions
The initial temperature $T_0(x)$ should reproduce the thermal state preceding the experiment. For uniformly conditioned specimens, $T_0(x) = T_i$ may be adopted. In experiments involving preheating, the use of a uniform profile may erase precisely the thermal memory that the model is intended to investigate.

The initial conversion $\alpha_0(x)$ will normally be zero for virgin material, unless there is evidence of ageing, prior decomposition, or thermal treatment. The initial position s0 defines the geometrical reference.

External Conditions and Unsteady Excitatio
Unsteadiness may be produced by variations in pressure, heat flux, gas temperature, or another operating condition. Time-dependent functions such as $p(t)$, $T_g(t)$, or $q_g(t)$ should therefore be recorded rather than only mean values.

The temporal resolution of the input data must be sufficiently fine to capture the characteristic response scale. An excessively filtered experimental signal may prevent identification of the true dynamics and lead to parameters that appear stable but are physically incorrect.

Preliminary Physical Scales
Before formal nondimensionalisation, it is useful to estimate characteristic length and time scales. For thermal diffusion, a characteristic depth may be approximated by $\ell_T \sim \sqrt{\kappa_s \tau}$,where τ denotes a time scale of interest [20]. Comparing ℓ_T with the domain depth helps determine the required numerical extent.

A regression time scale may be constructed from a reference rate giving $r_{\text{ref}}, \tau_r \sim L/r_{\text{ref}}$.Comparison among diffusive, kinetic, and regression scales anticipates the dimensionless groups to be established in Phase III.

Required Experimental Data
Calibration ideally requires measurements of regression rate, pressure, initial temperature,thermophysical properties, and kinetic information. Measurements of surface temperature or heat flux, when available, substantially improve the ability to distinguish competing mechanisms.

For validation, experiments not used for parameter identification should be reserved [13-28]. This separation is indispensable for assessing predictive capability and avoiding an apparently good performance that results merely from fitting the same data.

Identifiability and Uncertainty
Not all parameters can be determined simultaneously from a single observable. For example,changes in heat-transfer coefficients and interfacial energy terms may produce similar responses.Phase I therefore requires a preliminary assessment of which parameters are independently known, which will be calibrated, and which should remain fixed.

Identified parameters should be accompanied by uncertainty intervals or, at minimum, by sensitivity analysis. Experimental uncertainty must not be confused with structural model inadequacy.

Physical Admissibility Criteria
The solution should satisfy $T > 0$, $0 \le \alpha \le 1$, and a non-negative regression rate during sustained combustion. Properties such as k_S, c_S, and ρ_S must remain positive. Closure laws must not generate singularities within the operating range under consideration.

Beyond these bounds, the response should follow verifiable qualitative trends. A sustained increase in heat feedback should, under comparable conditions, increase the surface temperature; diffusion should smooth gradients; and the transformation should not spontaneously reverse under a simple irreversible kinetic law.

Limiting Cases for Verification
The physical architecture should recover elementary limiting cases: pure conduction without regression; heating with local kinetics but a fixed surface; prescribed regression; and steady operation under constant external conditions. These cases will be used to test the formulation and the code progressively.

Comparison with simple analytical or semi-analytical solutions, where available, should precede any application to complex data. A numerically sophisticated model cannot compensate for errors in signs, units, or boundary conditions.

Hierarchy of Complexity
Development will proceed incrementally. Level 1 considers constant properties, simple effective kinetics, and effective heat feedback. Level 2 may introduce temperature-dependent properties and radiation. Level 3 may incorporate multiple reactions, residual layers, or more detailed gas-phase coupling.

Progression from one level to the next should occur only when the data demonstrate that the preceding version is insufficient. This rule protects identifiability and keeps the model interpretable.

Physical Traceability Matrix

Mechanism	Principal quantities	Source of information
Thermal conduction	k_s, c_s, ρ_s, T	thermophysical tests and literature
Decomposition	A, E_a, n, α	thermal analysis and calibration
Regression	r, T_s, p	combustion experiments
Gas-phase feedback	q_g, h_g, T_g	measurement, correlation, or identification
Interface	L_{eff} and fluxes	energy balance
Initial state	T_0, α_0, s_0	experimental protocol

Phase I Deliverables

Deliverables
E1. Geometry and physical conventions. **E**2. Variables and parameters. **E3**. Assumptions and mechanisms. **E4**. Interfacial-balance architecture. **E5**. Required data and scales. **E6**. Verification criteria and requirements for progression to Phase II.

Conclusion of Phase I
Phase I establishes a traceable physical specification for the problem of unsteady solid-propellant combustion. The model is constructed around conduction, decomposition, regression, and heat feedback, with explicit attention to the moving boundary and thermal memory.

The principal methodological decision is to separate the physical definition from the mathematical formulation. Once the variables,

properties, signs, data, and mechanisms have been properly identified, Phase II can formulate the dimensional equations without introducing arbitrary terms and can transform the moving domain while preserving the meaning of each contribution.

PHASE II – Dimensional Formulation and Moving Boundary

Phase II Summary

Phase II converts the physical specification established in Phase I into a dimensional system of equations, initial conditions, and boundary conditions capable of representing thermal conduction, propellant decomposition, surface regression, and thermal feedback from the gas phase [29-37]. The central objective is to ensure that every term in the model has a physical meaning, consistent units, and an explicit connection to a previously identified mechanism.

The structural difficulty in this phase is the presence of the moving boundary $x = s(t)$ [4].

To prepare the analysis and numerical discretisation, a surface-attached coordinate is introduced, transforming the variable physical domain into a fixed domain. The transformation naturally generates an advective term associated with the regression velocity. This term does not represent material convection in the solid: it is a kinematic consequence of the coordinate transformation and must be retained to preserve equivalence between the two descriptions.

Principal outcome of Phase II
A closed and traceable dimensional model, accompanied by the transformation to surface-attached coordinates, initial and boundary conditions, sign conventions, dimensional verification, and the limiting-case tests required before nondimensionalisation.

Keywords: unsteady combustion; solid propellant; dimensional equations; moving boundary; moving coordinates; interfacial balance; surface regression.

Framework and Objectives of Phase II

Phase II inherits four principal variables from the preceding stage: temperature $T(x, t)$, degree of conversion $\alpha(x, t)$, surface position $s(t)$, and regression velocity $r(t) = -s^{\cdot}(t)$. It also inherits the thermophysical properties, kinetic parameters, external conditions, and the architecture of the interfacial energy balance. The task is now to transform these definitions into a dimensional mathematical formulation without introducing mechanisms that have not been physically justified.

The formulation must satisfy five objectives: conserve energy; represent thermal transformation; describe surface kinematics; establish an interfacial closure consistent with the adopted conventions; and produce an equivalent fixed-domain form. This sequence provides the basis for Phase III, in which dimensionless groups, dominant regimes, and comparison scales will be defined.

Formulation Principle
The problem is first written in the moving physical domain. Only then is the coordinate transformation performed. This order makes it possible to verify the origin of each term and reduces the risk of assigning an incorrect physical meaning to terms generated by the transformation.

Geometry, Orientation, and Sign Conventions

The x-axis is taken to be directed from the gas phase into the propellant. The instantaneous surface occupies the position $x = s(t)$ and the condensed phase corresponds to $x > s(t)$. During combustion, the surface recedes in the direction opposite to the positive axis; therefore the positive regression rate is defined by

$$r(t) = -\frac{ds}{dt}, \qquad r(t) \geq 0.$$

This convention allows r to be interpreted directly as the propellant consumption velocity. The surface temperature is $T_S(t) = T(s(t), t)$ and the conductive heat flux is defined according to Fourier's law. All interfacial conditions must respect this orientation in order to avoid sign reversals in the energy balance.

The deep boundary of the domain may be idealised by $x \to \infty$ or, in numerical calculations, truncated at $x = s(t) + L$. The value of L should be chosen so that the solution at the artificial boundary remains practically insensitive to surface heating over the simulation interval.

Dimensional Energy Equation in the Condensed Phase

For an effective homogeneous solid, with no macroscopic material motion in the physical coordinate, the minimal form of energy conservation is

$$\rho_s c_s \frac{\partial T}{\partial t} = \frac{\partial}{\partial x}\left(k_s \frac{\partial T}{\partial x}\right) + \dot{q}_{\text{chem}}(T, \alpha), \qquad x > s(t),\ t > 0.$$

If ρ_S, c_S, and ks are taken as constants, one obtains

$$\frac{\partial T}{\partial t} = \kappa_s \frac{\partial^2 T}{\partial x^2} + \frac{\dot{q}_{\text{chem}}}{\rho_s c_s}, \qquad \kappa_s = \frac{k_s}{\rho_s c_s}.$$

The term q_{chem} allows the volumetric thermal effect of decomposition to be represented when required. In the simplest version it may be set to zero, with decomposition retained only as a mechanism controlling conversion and the interface. This choice must be documented for each application.

Temperature-Dependent Properties

When the data show significant variation in the properties, the conservative form with $k_S(T)$ should be retained. Premature replacement by a constant diffusivity may introduce systematic error precisely in the near-surface region, where gradients and temperatures are greatest.

Dimensional Decomposition Equation

The variable α represents the transformed fraction of the material, with $0 \leq \alpha \leq 1$. An effective first-order kinetic law may be written as

$$\frac{\partial \alpha}{\partial t} = A \exp\left(-\frac{E_a}{R_u T}\right)(1 - \alpha)^n,$$

where A is the pre-exponential factor, E_a the activation energy, R_u the universal gas constant, and n the effective reaction order. This law constitutes a starting point rather than a universal prescription.

For multistep mechanisms, variables α_j and rates ω_j are introduced. The Phase II architecture should permit this extension without altering the fundamental thermal conservation law. If decomposition produces or consumes volumetric heat, one may use, for example,

$$\dot{q}_{\text{chem}} = \rho_s \sum_j Q_j \omega_j,$$

with the sign of Q_j defined consistently with the adopted energy convention.

Moving-Boundary Kinematics
The surface position is determined by

$$\frac{ds}{dt} = -r(t), \qquad s(0) = s_0.$$

The velocity $r(t)$ should not be imposed arbitrarily when the objective is to predict the transient response. It should result from a surface closure relation or from a mass and energy balance. A general form is

$$r(t) = \mathcal{R}(T_s(t), p(t), \alpha_s(t); \boldsymbol{\theta}_r),$$

where θ_r collects the regression parameters. This expression makes explicit that different laws may be tested within the same framework.

As a control reference, under steady conditions the solution may be compared with an empirical law of the form $r_{\mathrm{st}} = ap^m$. Such a comparison serves to verify the steady limit; it should not eliminate the transient dependence on T_S and the thermal history.

Interfacial Energy Balance
At the surface $x = s(t)$, the thermal feedback from the gas phase must balance conduction into the solid and the energetic effects associated with regression. A general dimensional form is

$$q_g(t) - q_{\mathrm{rad,out}}(t) = k_s \left.\frac{\partial T}{\partial x}\right|_{s^+} + \rho_s r(t) L_{\mathrm{eff}},$$

where L_{eff} represents an effective energy per unit mass associated with interfacial processes. The exact form and signs should be confirmed against the operational definition of each flux.

A simple thermal closure for the gas side may be

$$q_g = h_g\,[T_g(t) - T_s(t)],$$

with a radiative term added when necessary. The value of h_g may be prescribed from independent data or identified within physically admissible bounds.

Mandatory Interface Verification
The sum of the terms in the balance must have units of heat flux, $\mathrm{Wm^{-2}}$. In addition, an increase in gas-phase thermal feedback, with the remaining conditions unchanged, should produce a physically consistent surface thermal response.

Initial Conditions and Deep-Boundary Condition
At the initial instant, one specifies

$$T(x,0) = T_0(x), \qquad \alpha(x,0) = \alpha_0(x), \qquad s(0) = s_0.$$

For an initially uniform propellant, $T_0(x) = T_i$ and $\alpha_0(x) = 0$ may be adopted. However, preheated tests should use the actual prepared thermal profile, since the initial thermal memory may appreciably alter ignition delay and the transient response.

In the deep interior one may impose

$$T(x,t) \to T_i \quad \text{quando} \quad x - s(t) \to \infty.$$

In a truncated domain $0 \le \xi \le L$, this condition is replaced by $T(L, t) = T_i$ or, when physically more appropriate, by an approximately zero-flux condition. Independence of the solution with respect to L should be tested numerically.

Transformation to Surface-Attached Coordinates
Define the moving coordinate

$$\xi = x - s(t), \qquad \xi \ge 0,$$

and the new functions

$$\Theta(\xi, t) = T(x,t), \qquad A_c(\xi, t) = \alpha(x,t).$$

The surface then permanently occupies $\xi = 0$. Since $x = \xi + s(t)$, the chain rule gives, for a generic quantity $f(x,t) = F(\xi,t)$,

$$\left.\frac{\partial f}{\partial t}\right|_x = \left.\frac{\partial F}{\partial t}\right|_\xi - \dot{s}(t)\frac{\partial F}{\partial \xi} = \frac{\partial F}{\partial t} + r(t)\frac{\partial F}{\partial \xi},$$

and

$$\frac{\partial f}{\partial x} = \frac{\partial F}{\partial \xi}.$$

This identity is the central step of Phase II. The term proportional to r arises solely because the reference frame follows the regressing surface.

Transformed System in a Fixed Domain
For constant properties, the thermal equation becomes

$$\rho_s c_s \left(\frac{\partial \Theta}{\partial t} + r\frac{\partial \Theta}{\partial \xi}\right) = k_s \frac{\partial^2 \Theta}{\partial \xi^2} + \dot{q}_{\mathrm{chem}}(\Theta, A_c).$$

Equivalently,

$$\frac{\partial \Theta}{\partial t} = \kappa_s \frac{\partial^2 \Theta}{\partial \xi^2} - r\frac{\partial \Theta}{\partial \xi} + \frac{\dot{q}_{\mathrm{chem}}}{\rho_s c_s}.$$

The conversion equation becomes

$$\frac{\partial A_c}{\partial t} + r\frac{\partial A_c}{\partial \xi} = A \exp\!\left(-\frac{E_a}{R_u \Theta}\right)(1 - A_c)^n.$$

The system is then solved on a fixed spatial domain, while information about the motion remains embedded in the terms proportional to $r(t)$ and in the kinematic equation for $s(t)$.

Interpretation of the Transport Term
The term $-r\Theta_\xi$ in the evolutionary form does not mean that the solid has a physical convective velocity equal to $-r$. It represents the apparent transport of the profile when observed from the moving surface. This distinction is important both for interpreting the results and for selecting the numerical method.

Boundary Conditions in the Transformed Domain
In the new coordinate, the surface temperature is simply $\Theta(0, t) = T_S(t)$. The energy balance takes the form

$$q_g(t) - q_{\mathrm{rad,out}}(t) = k_s \left.\frac{\partial \Theta}{\partial \xi}\right|_{0^+} + \rho_s r(t) L_{\mathrm{eff}}.$$

At the deep limit, $\Theta(\xi, t) \to T_i$ as $\xi \to \infty$. In a truncated domain, the selected condition is imposed at $\xi = L$.

The advantage of this formulation is operational: the spatial mesh may remain fixed relative to the interface. The surface does not cross mesh cells, which simplifies calculation of the surface gradient, coupling with the regression law, and imposition of the boundary conditions.

Compact Form of the Coupled Problem
The baseline model may be summarised as

$$\begin{cases} \Theta_t = \kappa_s \Theta_{\xi\xi} - r\Theta_\xi + \dot{q}_{\text{chem}}/(\rho_s c_s), \\ (A_c)_t = \omega(\Theta, A_c) - r(A_c)_\xi, \\ \dot{s} = -r, \\ r = \mathcal{R}(\Theta(0,t), p(t), A_c(0,t); \boldsymbol{\theta}_r), \end{cases}$$

with the associated interfacial balance, deep-boundary condition, and initial data. This form highlights the coupled nature of the problem: temperature affects kinetics and regression; regression alters the apparent transport; and the surface balance in turn constrains the temperature.

Minimum Closed Structure

The system is mathematically closed only when the regression law, gas-phase heat flux, kinetic parameters, interfacial balance, and all initial and boundary conditions have been defined. An isolated thermal equation does not yet constitute the complete model.

Dimensional Verification

Verification of units must precede any implementation [32,33]. In the thermal equation, the terms $\rho_S\ c_S\ T_t$, $k_S\ Txx$, and q_{chem} must share the units of power per unit volume. In the kinetic equation, both sides must have dimensions of inverse time when α is dimensionless.

Quantity	SI Unit	Role in the Model
ρ_s	kgm^{-3}	propellant density
c_s	$\text{J kg}^{-1}\ \text{K}^{-1}$	thermal storage
k_s	$\text{Wm}^{-1}\ \text{K}^{-1}$	thermal conduction
k_s	$\text{m}^2\ \text{s}^{-1}$	thermal diffusivity
r	ms^{-1}	regression velocity
q_g	Wm^{-2}	gas-phase thermal feedback
L_{eff}	J kg^{-1}	interfacial energetic effect
A	s^{-1}	effective kinetic scale
E_a	J mol^{-1}	activation energy

Limiting-Case Tests of the Formulation

Before discretisation, the formulation must recover simple cases. If $r = 0$ and $q_{\text{chem}} = 0$, the classical heat-conduction equation must result. If the temperature is uniform and conduction vanishes, the evolution of α must reduce to the local kinetic law. If the external conditions remain constant for sufficiently long, the solution should approach a steady regime compatible with the selected closure.

Another important test is to compare the solution written in physical coordinates with the transformed solution for a case in which r is prescribed and simple. The two descriptions must coincide after transformation back to the original coordinates. This test verifies the sign and implementation of the transport term generated by the moving boundary.

Aspects of Existence, Regularity, and Physical Admissibility

Detailed mathematical analysis will be developed at a later stage, but Phase II must already impose admissibility conditions. One expects $T > 0$, $0 \le A_C \le 1$, and $r \ge 0$ in the combustion regime. Closure functions must avoid singularities within the physical operating range, and parameters must lie within intervals compatible with independent data.

For positive and sufficiently regular properties, the thermal part retains its parabolic character. Nonlinear coupling enters through the kinetics, surface balance, and regression law. This structure suggests that stability and positivity should be preserved by the discretisation rather than treated merely as a posteriori checks.

Preparation for Numerical Implementation

The transformation to ξ makes it possible to construct a fixed mesh $0 = \xi_0 < \xi_1 < \cdots < \xi_N = L$. Conduction may be discretised by finite differences, finite volumes, or finite elements. The transport term associated with r requires particular attention when regression becomes rapid relative to diffusion, since a simple centred discretisation may produce non-physical oscillations.

Time integration must resolve the coupling among the thermal field, kinetics, and interface. An initial strategy is to use an implicit or semi-implicit method for diffusion, update the kinetics in a stable manner, and iterate the interfacial condition within each time step. The definitive choice belongs to the numerical phase; at this stage only the requirements to be respected by the algorithm are established.

Phase II Traceability Matrix

Physical element	Mathematical representation	Principal verification
Thermal storage	$\rho_S\ c_S\ T_t$	units and conservation
Conduction	$(k_S T_X)x$	classical diffusive limit
Decomposition	$\alpha_t = \omega(T, \alpha)$	$0 \le \alpha \le 1$
Regression	$s^{\cdot} = -r$	sign and physical monotonicity
Gas-phase feedback	q_g	interfacial balance
Moving boundary	$\xi = x - s(t)$	equivalence between domains
Thermal memory	field $\Theta(\xi, t)$	response to disturbances

Phase II Execution Plan

This phase should be executed in an order that preserves traceability [31]:

1. finalise the geometric and sign conventions;
2. write the dimensional equations in the moving physical domain;
3. define the kinetic, regression, and thermal-feedback laws;
4. close the interfacial balance and the initial and deep-boundary conditions;
5. perform the transformation $\xi = x - s(t)$ and verify the chain rule;
6. confirm units, simple limits, and physical admissibility;
7. prepare the formulation for nondimensionalisation and discretisation.

Phase II Deliverables

E1. Dimensional system in the moving domain. **E2**. Interfacial energy balance. **E3**. Transformation to a fixed domain. **E4**. Complete transformed system. **E5**. Table of units and limiting-case tests. **E6**. Transition document for Phase III.

Transition Document for Phase III

Phase III should receive a closed dimensional system on the domain $0 \le \xi \le L$, with all quantities and parameters defined. The next task will be to select reference scales for temperature, length, time, velocity, heat flux, and pressure, introduce

dimensionless variables, and identify the groups governing the competition among diffusion, regression, kinetics, and external forcing.

Nondimensionalisation should not alter the physical structure established in this phase. On the contrary, it should reveal which terms dominate in different regimes and provide quantitative criteria for simplification. The resulting groups should also guide the selection of mesh resolution, time step, and experimental sets for calibration and validation.

Conclusion of Phase II

The second phase transforms the physical specification of Phase I into a coherent dimensional formulation. The thermal field, conversion, regression, and surface balance become part of a single coupled system in which each term can be related to a property, mechanism, or experimental condition.

The transformation $\xi = x - s(t)$ is the central technical result. It fixes the surface at $\xi = 0$ and transfers the effect of motion to apparent transport terms. In this way, the physics of the moving boundary is preserved while simultaneously obtaining a geometry suitable for mathematical analysis and computational implementation.

The resulting formulation is ready for the next stage: nondimensionalisation and analysis of the dominant regimes. Before that transition, the signs in the interfacial balance, the units of all parameters, and the equivalence between the physical and transformed descriptions must be confirmed.

PHASE III – Nondimensionalisation and Dominant Regimes

Phase III Summary

Phase III transforms the closed dimensional system established in Phase II into a dimensionless formulation designed to reveal the dynamic structure of the problem. The purpose is not merely to reduce the apparent number of parameters, but to identify physically meaningful combinations capable of comparing thermal diffusion, apparent transport due to regression, decomposition kinetics, thermal feedback, and interfacial effects.

The reference scales are selected in a traceable manner. Each dimensional variable is assigned a reference quantity with a physical interpretation and, whenever possible, a measurable counterpart. The resulting system makes it possible to identify dominant regimes, establish criteria for controlled simplifications, and prepare the mathematical analysis, numerical implementation, and experimental design.

Principal outcome of Phase III
A complete dimensionless system, accompanied by the governing dimensionless groups, the physical interpretation of each group, limiting regimes, and criteria for mesh selection, time-step selection, calibration, and validation.

Keywords: nondimensionalisation; Péclet number; Damköhler number; Biot number; Arrhenius kinetics; regression; thermal memory; dominant regimes.

Objectives and Similarity Principle

Nondimensionalisation replaces unit-dependent quantities with ratios of characteristic scales. Two geometrically similar experiments may exhibit comparable dynamic behaviour when the relevant dimensionless groups take similar values, even if their dimensions, characteristic times, or absolute heat-flux levels differ.

Four objectives are pursued in this phase: to reduce parametric redundancy; quantify the relative importance of the mechanisms; identify useful asymptotic limits; and construct variables suitable for comparisons among experiments, simulations, and materials.

Traceability rule
No dimensionless group is introduced solely for algebraic convenience. Each combination must be associated with a ratio of scales, a physical mechanism, or a boundary condition of the dimensional model.

Reference Scales

A characteristic length L, a reference temperature T_i, and a temperature difference $\Delta T = T_{\text{ref}} - T_i > 0$ are selected. The diffusive time scale is

$$t_d = \frac{L^2}{\kappa_s},$$

and the associated diffusive velocity is $u_d = \kappa_S/L$. A reference velocity rref is adopted for regression; $q_{\text{ref}} = k_S\ \Delta T/L$ for heat flux; and a value pref representative of the experimental range for pressure.

The choice of L should reflect the thermally active thickness or the depth of the truncated domain. The choice of ΔT should avoid excessively small values, since these would artificially amplify the dimensionless coefficients.

Dimensionless Variables

We introduce

$$X = \frac{\xi}{L}, \qquad \tau = \frac{t}{t_d}, \qquad \theta = \frac{\Theta - T_i}{\Delta T}, \qquad a = A_c,$$

$$R = \frac{r}{r_{\text{ref}}}, \qquad P = \frac{p}{p_{\text{ref}}}, \qquad S = \frac{s - s_0}{L}.$$

The surface remains at $X = 0$, and the truncated domain may be represented by $0 \le X \le 1$. The conversion variable is already naturally dimensionless and retains the physical interval $0 \le a \le 1$.

Dimensionless Thermal Equation

For constant properties, and writing the chemical source as $q_{\text{chem}} = Q_V\ \omega(\Theta, a)$, the transformed equation from Phase II gives

$$\theta_\tau = \theta_{XX} - Pe_r\, R\, \theta_X + \Omega_T(\theta, a),$$

where

$$Pe_r = \frac{r_{\text{ref}} L}{\kappa_s}$$

is the Péclet number associated with regression. The term Ω_T represents the dimensionless chemical source, whose amplitude depends on the kinetic scale and the effective heat of transformation.

When $Pe_r \ll 1$, thermal diffusion dominates the apparent transport produced by interface motion. When Pe_r is of order unity or larger, regression significantly alters the shape and relative position of the thermal profile in the surface-attached frame.

Dimensionless Kinetics and Arrhenius Parameter

For the law

$$\omega = A \exp\left(-\frac{E_a}{R_u \Theta}\right)(1 - a)^n,$$

the thermal Damköhler number is defined as

$$Da = A\,t_d = A\frac{L^2}{\kappa_s}$$

and the activation parameter as

$$\beta = \frac{E_a}{R_u T_{\text{ref}}}.$$

Since $\Theta = T_i + \Delta T\,\theta$, the conversion equation may be written as

$$a_\tau + Pe_r R\,a_X = Da\,\exp\left[-\frac{E_a}{R_u(T_i + \Delta T\theta)}\right](1-a)^n.$$

This form exactly preserves the dimensional temperature dependence. A subsequent reparameterisation may use ratios such as T_i/T_{ref} and $\Delta T/\text{T}_{\text{ref}}$ to make the exponential sensitivity explicit.

Dimensionless Interfacial Balance
Taking $q_{\text{ref}} = k_S\Delta T/L$, define

$$Q_g = \frac{q_g}{q_{\text{ref}}}, \qquad Q_{rad} = \frac{q_{\text{rad,out}}}{q_{\text{ref}}}.$$

The interfacial balance becomes

$$Q_g - Q_{rad} = \theta_X|_{0^+} + \Lambda\,Pe_r R,$$

where

$$\Lambda = \frac{\rho_s L_{\text{eff}}}{\rho_s c_s \Delta T} = \frac{L_{\text{eff}}}{c_s \Delta T}$$

measures the effective interfacial energy relative to the sensible energy associated with ΔT. This form highlights the competition among incoming heat, conduction into the interior, and energy associated with surface consumption.

Effective Biot Number
If gas-phase thermal feedback is approximated by $q_g = h_g(Tg - T_S)$, the following group arises naturally

$$Bi_g = \frac{h_g L}{k_s}.$$

The effective Biot number compares internal conductive resistance with heat transfer at the interface. Small values indicate relatively weak surface transfer, whereas large values make the internal field and near-surface gradients particularly important.

The simultaneous presence of Bi_g, Pe_r, and Λ shows that a change in surface temperature may result from distinct mechanisms. This observation will be important in the parameter-identifiability analysis.

Dimensionless Regression Law
A general law from Phase II,

$$r = \mathcal{R}(T_s, p, a_s; \boldsymbol{\theta}_r),$$

becomes

$$R = \mathcal{R}^*(\theta_s, P, a_s; \boldsymbol{\Pi}_r),$$

where Πr collects the dimensionless parameters of the selected law. If a reference law of the form $r = Cp^m$ is used, the convenient choice $r_{\text{ref}} = Cp_{\text{ref}}^m$ yields R = Pm in the corresponding limit.

This normalisation separates the absolute regression scale from pressure sensitivity and facilitates comparison among materials or experimental campaigns.

Dimensionless Surface Kinematics
From $s^{\cdot} = -r$, one obtains

$$\frac{dS}{d\tau} = -Pe_r R.$$

Thus, the same group Pe_r that appears in the apparent transport term controls how rapidly the dimensional surface position changes relative to the diffusive time scale. This recurrence is not coincidental: both effects arise from the same regression kinematics.

Compact Dimensionless System
The minimum structure may be summarised as

$$\begin{cases} \theta_\tau = \theta_{XX} - Pe_r R\theta_X + \Omega_T(\theta, a), \\ a_\tau = \Omega_a(\theta, a) - Pe_r R a_X, \\ S_\tau = -Pe_r R, \\ R = \mathcal{R}^*(\theta(0,\tau), P(\tau), a(0,\tau); \boldsymbol{\Pi}_r), \end{cases}$$

together with the dimensionless interfacial balance and the corresponding initial and deep-boundary conditions. The function Ω_a contains the factor Da and the Arrhenius sensitivity, whereas Ω_T contains the energetic coupling of decomposition.

Primary Structural Groups
Pe_r measures regression relative to diffusion; Da measures kinetics relative to diffusion; Bi_g measures gas-phase heat transfer relative to internal conduction; Λ measures interfacial energy relative to sensible heating; and β measures the strength of Arrhenius sensitivity.

Matrix of Dimensionless Groups

Group	Definition	Interpretation
Pe_r	$r_{\text{ref}}L/\kappa_s$	regression versus thermal diffusion
Da	AL^2/κ_s	kinetics versus diffusive time
Bi_g	$h_g L/k_s$	thermal feedback versus internal conduction
Λ	$L_{\text{eff}}/(c_s\Delta T)$	interfacial energy versus sensible heat
β	$E_a/(R_u T_{\text{ref}})$	thermal sensitivity of the kinetics
P	p/p_{ref}	normalised pressure forcing

Dominant Regimes
The combination of these groups organises the operating space. For $Pe_r \ll 1$, diffusion rapidly reorganises the profile compared with surface displacement. For $Pe_r \gtrsim 1$, regression kinematics cannot be treated as a small perturbation. For $Da \ll 1$, decomposition is slow on the diffusive time scale; for $Da \gg 1$, the reaction may become concentrated within a narrow thermal region and require enhanced spatial and temporal resolution.

Large values of Bi_g strengthen the coupling between the gas-phase condition and the surface, whereas large Λ indicates that a substantial fraction of the available flux may be consumed by the

interfacial energy term. Interpretation should nevertheless be based on the set of groups rather than on any single number in isolation.

Thermal Memory in Dimensionless Form

Thermal memory remains embedded in the field $\theta(X, \tau)$. Following a pressure or heat-flux disturbance, the surface may respond rapidly, while the interior retains the signature of the previous state for a finite interval. The natural scale for this persistence is the diffusive time t_d.

For comparison of transient experiments, it is useful to express the forcing as a function of τ and measure delays or relaxation times on the same scale. Responses with different dimensional durations may then reveal similar dynamics when the governing groups are comparable.

Criteria for Controlled Simplifications

A simplification should be adopted only after it has been justified by scale analysis. If Pe_r is consistently very small, the apparent transport term may be tested as a perturbation. If the volumetric chemical source is negligible relative to conduction and the surface balance, it may be removed from the thermal equation while retaining the kinetics as an auxiliary variable. If radiation is small relative to q_{ref}, it may be treated as a correction.

These reductions must be validated against the complete model over a representative parameter range. Nondimensionalisation provides the quantitative criteria required to determine when an approximation is justified.

Implications for Numerical Discretisation

The mesh must resolve the smallest relevant spatial scales. As Pe_r increases, the transport term requires stable schemes and may justify upwind treatment, stabilisation, or high-resolution methods. When Da and β are large, the kinetics may become stiff, favouring implicit or adaptive time integration.

The dimensionless time step $\Delta\tau$ should be selected according to the stability and accuracy requirements of the chosen method. Even with unconditionally stable implicit schemes, excessively large steps may suppress the transient response that constitutes one of the central objects of the project.

Implications for Calibration and Experiments

Dimensionless analysis helps to select informative experiments. Tests concentrated within a narrow range of Pe_r, Da, or Bi_g may fail to separate parameter effects adequately. It is preferable to design campaigns that span different regimes while remaining within the safety limits and validity domain of the model.

Calibration should distinguish independently known dimensional parameters from inferred parameters. Results may be reported both in physical units and in terms of the dimensionless groups, allowing assessment of whether different parameter sets lead to dynamically equivalent regimes.

Phase III Consistency Tests

The transformation must be reversible: a dimensionless solution converted back to physical units must satisfy the Phase II system within numerical error. Every term in the dimensionless equations must genuinely be dimensionless, and limiting cases must reproduce the expected reductions.

Unit-invariance tests must also be performed. Changing from metres to millimetres, or from seconds to another coherent unit, must not alter Pe_r, Da, Bi_g, Λ, or the dimensionless results.

Phase III Execution Plan

This phase should be executed in the following sequence:

1. define L, T_i, ΔT, t_d, r_{ref}, q_{ref}, and p_{ref};
2. introduce the dimensionless variables and substitute them into the Phase II system;
3. identify and name the governing dimensionless groups;
4. rewrite the initial, deep-boundary, and interfacial conditions;
5. verify reversibility, units, and limiting cases;
6. map the regimes relevant to the available experimental data;
7. produce quantitative requirements for the subsequent numerical phase.

Phase III Deliverables
E1. Reference Scales justificadas. **E2**. Complete dimensionless system. **E3**. Matrix of dimensionless groups. **E4**. Conceptual map of dominant regimes. **E5**. Simplification and discretisation criteria. **E6**. Transition document for Phase IV.

Transition Document for Phase IV

Phase IV should receive both the dimensional and dimensionless systems, together with plausible ranges of the governing groups. The next stage may then focus on discretisation, the coupling algorithm, convergence tests, and computational verification against limiting cases.

The implementation must preserve positivity, conversion bounds, and energetic consistency. Convergence analysis should distinguish spatial, temporal, and iterative errors from model-form error and parameter uncertainty.

Conclusion of Phase III

The third phase reorganises the model in terms of characteristic scales and physical ratios. Thermal diffusion provides the temporal and spatial reference, while Pe_r, Da, Bi_g, Λ, and β characterise regression, kinetics, gas-phase heat transfer, interfacial energy demand, and thermal sensitivity, respectively.

This formulation permits comparison of experimental conditions independently of the units employed, identification of regimes in which particular mechanisms dominate, and establishment of objective criteria for simplification. Nondimensionalisation does not replace the dimensional model; it complements it by making the hierarchy of processes more transparent.

With Phase III completed, the project possesses a coherent chain extending from the physical specification through the dimensional equations to the dimensionless structure. The next stage can therefore be devoted to constructing and verifying the numerical method without losing the physical traceability established since Phase I.

PHASE IV – Discretisation, Algorithm and Numerical Verification

Phase IV Summary

Phase IV transforms the dimensionless system established in Phase III into a verifiable computational procedure. The objective is not merely to obtain numerical solutions but to construct a computational chain in which spatial discretisation, time integration, thermochemical coupling, the regression law, and the interfacial balance can be tested both separately and jointly.

Principal Outcome of Phase IV

A complete numerical scheme for θ(X, τ), a(X, τ), R(τ), and S(τ), accompanied by a coupling algorithm, stability and convergence criteria, conservation tests, and a computational verification protocol.

Numerical Objectives

The implementation must preserve the physical structure defined in the preceding phases. In particular, it should ensure finite θ, $0 \le a \le 1$, $R \ge 0$ in the combustion regime, and consistency of the interfacial energy balance. The solution must converge as the mesh and time step are refined and must recover limiting cases for which analytical or semi-analytical solutions, or known asymptotic behaviour, are available.

The first implementation will be one-dimensional, on the fixed domain $0 \le X \le 1$. This choice allows verification to focus on the essential mechanisms before more complex geometries, kinetics, or gas-phase couplings are introduced.

Spatial Mesh and Discrete Representation

Consider a uniform mesh

$$X_i = i\,\Delta X, \qquad i = 0, 1, \ldots, N, \qquad \Delta X = \frac{1}{N},$$

and time levels τ^n with step $\Delta\tau = \tau^{n+1} - \tau^n$. The nodal approximations are denoted by $\theta_i^n \approx \theta(X_i, \tau^n)$ and $a_i^n \approx a(X_i, \tau^n)$.

For thermal diffusion, a second-order central difference is initially adopted [30],

$$\theta_{XX}\big|_i \approx \frac{\theta_{i+1} - 2\theta_i + \theta_{i-1}}{(\Delta X)^2}.$$

The transport term associated with regression requires a treatment consistent with the sign of R. For $R \ge 0$, a first-order upwind approximation provides robustness during the initial development stage; a second-order version may be introduced after the baseline tests have been completed.

Time Discretisation

The potential stiffness produced by large Da and Arrhenius sensitivity favours an implicit or semi-implicit method. Backward Euler is proposed as the reference scheme for diffusion and the stiff terms, while retaining the possibility of subsequent comparison with Crank–Nicolson or BDF methods [34].

In schematic form, the thermal equation is written as

$$\frac{\theta_i^{n+1} - \theta_i^n}{\Delta\tau} = D_{XX}\theta_i^{n+1} - Pe_r R^{n+1} D_X^{\mathrm{up}}\theta_i^{n+1} + \Omega_T(\theta_i^{n+1}, a_i^{n+1}),$$

whereas the conversion variable satisfies

$$\frac{a_i^{n+1} - a_i^n}{\Delta\tau} + Pe_r R^{n+1} D_X^{\mathrm{up}} a_i^{n+1} = \Omega_a(\theta_i^{n+1}, a_i^{n+1}).$$

This formulation generally leads to a nonlinear system at each time step.

Treatment of the Interface

At the surface node $X_0 = 0$, the balance

$$Q_g - Q_{rad} = \theta_X(0, \tau) + \Lambda Pe_r R$$

must be discretised with an order of consistency compatible with that adopted in the interior. A second-order one-sided approximation may be used for the gradient,

$$\theta_X(0) \approx \frac{-3\theta_0 + 4\theta_1 - \theta_2}{2\Delta X}.$$

The regression law is evaluated using the updated surface values. In this manner, surface temperature, heat flux, and regression velocity are solved as coupled quantities rather than as independent inputs.

Deep-Boundary Condition

For a sufficiently extended truncated domain, one may impose $\theta_N = 0$, corresponding to the reference initial temperature. Alternatively, a zero-flux condition may be tested when the deep boundary represents a thermally undisturbed region. The effective boundary distance must be verified through a domain-independence study: increasing L should not significantly alter the solution in the active region.

Coupling Algorithm

At each time step, the following sequence is proposed:

1. use the solution at time τ^n as the initial estimate;
2. update the regression law using θ_0, a_0, and P;
3. solve the implicit thermal and kinetic system;
4. recompute the interfacial balance and R;
5. iterate until the changes in θ, a, and R fall below the prescribed tolerances;
6. update $S^{n+1} = S^n - \Delta\tau\, Pe_r R^{n+1}$;
7. apply admissibility and conservation tests before advancing.

For moderate nonlinearities, Picard iteration may be sufficient. In strongly activated regimes, a Newton method, with damping where necessary, should reduce the number of iterations and improve robustness.

Iterative Convergence Criterion

An initial choice is to require simultaneously $\|\theta^{(k+1)} - \theta^{(k)}\|\infty < \varepsilon_T$, $\|a^{(k+1)} - a^{(k)}\|\infty < \varepsilon_a$, and $|R^{(k+1)} - R^{(k)}| < \varepsilon_R$. The tolerances should be smaller than the discretisation error that is to be measured.

Stability, Positivity and Physical Bounds

Although an implicit scheme alleviates the classical diffusive stability restrictions, $\Delta\tau$ remains constrained by accuracy and by the need to resolve transients. Excessive temperature increments, spurious oscillations, and violations of $0 \le a \le 1$ must be monitored.

Artificial enforcement of bounds by clipping should be used only as an emergency safeguard, because it may conceal algorithmic deficiencies. The objective is to select the discretisation, time step, and nonlinear solver so that the physical bounds are preserved by the numerical dynamics themselves.

Verification through Progressive Test Cases

Verification will proceed from simple to fully coupled problems. First, pure conduction without regression or reaction is solved and compared with a known solution. The transport term with prescribed R is then introduced. Local kinetics at prescribed temperature are tested next. Only thereafter are the kinetics, interfacial balance, and regression law activated simultaneously.

This strategy allows implementation errors to be localised. A discrepancy in the fully coupled model should not be investigated before the elementary subproblems have passed their respective tests.

Mesh-Convergence Study

Following established numerical verification practices, at least three successive spatial resolutions will be used, for example N, $2N$, and $4N$, combined with consistent temporal refinement [11,12]. For a quantity of interest ϕ, the difference between resolution levels is defined and the observed order is estimated from the error ratio.

The analysis must include surface temperature, regression velocity, interface position, and internal profiles at selected times. Convergence of a single variable is not sufficient to declare the system numerically verified.

Numerical Example in MATLAB – Mesh Convergence

As an illustrative example, consider three meshes with N = 50, 100, and 200 nodes and calculated values of the maximum surface temperature θs,max = 1.2840, 1.3015, and 1.3061. The following MATLAB code estimates the observed order p for a refinement ratio r = 2 and a Richardson extrapolation of the quantity of interest. The values are illustrative only and should be replaced by results from the complete model.

```
N = [50 100 200];
phi = [1.2840 1.3015 1.3061];
r = 2;
e21 = phi(2) - phi(1);
e32 = phi(3) - phi(2);
p = log(abs(e21/e32))/log(r);
phi_ext = phi(3) + (phi(3)-phi(2))/(r^p-1);
err_rel = abs((phi_ext-phi(3))/phi_ext)*100;
fprintf('p = %.3f\\n',p);
fprintf('Richardson = %.6f\\n',phi_ext);
fprintf('Relative error = %.3f %%\\n',err_rel);

figure;
plot(1./N,phi,'o-','LineWidth',1.4);
hold on;
yline(phi_ext,'--','Richardson extrapolation');
xlabel('Inverse mesh size, 1/N');
ylabel('Maximum surface temperature, \\theta_{s,max}');
title('Mesh-convergence behaviour');
grid on;
```

For these illustrative data, $p \approx 1.93$ is obtained, consistent with a trend close to second-order convergence. The Richardson estimate is $\theta^{ext}s$,max ≈ 1.3077, and the finest-grid relative discretisation error is about 0.12%. The extrapolation therefore supplies a quantitative reference against which the N = 200 computation can be assessed before physical calibration.

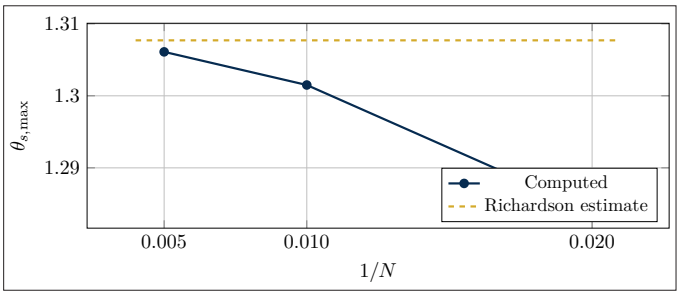


Figure 1: Approximate Mesh-Convergence Graph for the Matlab Example. The Computed Maximum Surface Temperature Approaches the Richardson-Extrapolated Value as the Mesh Is Refined

Discrete Energy Balance

In addition to convergence, an energy residual must be calculated. The energy received at the interface, less losses, conducted energy, energy associated with transformation, and the change in stored energy should tend to zero as ΔX and $\Delta\tau$ decrease.

This test is particularly important because a visually smooth solution may still contain a systematic error in boundary coupling. The residual will be reported both in absolute form and normalised by the reference heat flux.

Reference Transient Tests

The unsteady response will be tested using controlled perturbations of $P(\tau)$ or $Qg(\tau)$: step, pulse, and smooth variations. For each test, $\theta_S(\tau)$, $R(\tau)$, $S(\tau)$, and temperature and conversion profiles will be recorded.

These tests make it possible to observe delay, relaxation, and thermal memory. Comparisons among different Pe_r, Da, Big, Λ, and β should qualitatively reproduce the regimes predicted in Phase III.

Computational Architecture

The implementation should separate modules for input data, properties, kinetics, gas-phase heat flux, regression law, system assembly, nonlinear solver, time control, diagnostics, and result export. This separation reduces dependencies and facilitates replacement of constitutive models.

Each run must store the parameters, code version, mesh, tolerances, convergence status, and diagnostic quantities. Numerical reproducibility is treated as part of the scientific method rather than as a subsequent task.

Phase IV Acceptance Criteria

The phase will be considered complete when the elementary tests reproduce the selected references; mesh refinement demonstrates convergence; the discrete energy-balance residual decreases with refinement; the physical bounds are respected; and the algorithm solves, without artificial instability, at least a representative set of regimes defined in Phase III.

Results that depend strongly on ΔX, $\Delta\tau$, or the iterative tolerances will not be used for physical calibration until the numerical dependence has been brought under control.

Phase IV Execution Plan

1. implement pure conduction and validate the diffusive operator;
2. add regression-induced transport and test the upwind scheme;
3. implement the kinetics and verify the conversion bounds;
4. discretise the interfacial balance and the regression law;
5. construct the nonlinear coupling cycle;
6. perform mesh, time-step, and tolerance studies;
7. execute the reference transient tests;
8. document errors, residuals, and acceptance criteria.

Phase IV Deliverables
E1. Complete discrete formulation. **E2**. Coupling algorithm. **E3**. Set of unit tests and reference cases. **E4**. Spatial and temporal convergence study. **E5**. Energy-balance and admissibility report. **E6**. Specification for calibration, validation, and parametric analysis in the subsequent phase.

Conclusion of Phase IV

Phase IV establishes the bridge between the physico-mathematical model and computational simulation. The use of a fixed domain, finite differences, implicit treatment, and iterative coupling provides a transparent basis that is sufficiently robust for the first implementation and suitable for systematic convergence studies.

The central aspect of this stage is verifiability. The code must demonstrate that it correctly solves the formulated equations before it is confronted with experimental data. Accordingly, convergence, conservation, admissibility, and recovery of limiting cases are treated as outcomes of the phase rather than as mere programming details.

With Phases I–IV completed, the project has a physical foundation, a dimensional system, a dimensionless structure, and a verifiable numerical method. The subsequent phase can therefore focus on parameter calibration, experimental validation, sensitivity analysis, and uncertainty quantification.

PHASE V – Calibration, Experimental Validation and Uncertainty Quantification

Phase V Summary

Phase V confronts the numerically verified model with experimental data and establishes the extent to which the parameters can be identified, the predictions validated, and uncertainty quantified. This stage explicitly separates calibration from validation: data used to estimate parameters are not reused as the sole evidence of predictive capability [12,17].

Main Product of Phase V
A reproducible calibration and validation protocol, with separate datasets, an objective function, identifiable parameters, sensitivity analysis, error metrics, uncertainty bands, and acceptance criteria for the model's intended application domain.

Objectives of Phase V

This phase has five objectives: to estimate parameters that cannot be measured directly; assess parameter identifiability and correlation; validate the model against independent experiments; quantify the sensitivity of responses to inputs; and propagate uncertainties to the quantities of interest. The expected outcome is not merely a set of parameter values, but a quantitative characterisation of the confidence that can reasonably be assigned to the predictions.

Organisation of Experimental Data

The data will be divided into calibration and validation sets before final fitting. Each test should retain metadata on the propellant, geometry, initial temperature, pressure, instrumentation, acquisition frequency, measurement uncertainty, and signal processing. Wherever possible, validation will use conditions different from those employed for calibration, while remaining within the intended application domain.

Data traceability is essential. Removed, filtered, or corrected values must be identified and justified. Instrumental uncertainty and variability among repeated tests should be recorded separately so that the entire discrepancy is not attributed to the model [12].

Parameters to Be Calibrated

Calibration should focus on parameters that are difficult to measure independently and for which the data contain sufficient information. Candidate quantities include effective heat-feedback coefficients, regression-law parameters, kinetic factors, and interfacial energy terms. Thermophysical properties that are well established experimentally should preferably be fixed or represented by narrow distributions rather than introduced as additional degrees of freedom.

Before fitting, a parameter–observable matrix will be constructed. If two parameters produce practically indistinguishable effects on all measured quantities, their simultaneous estimation will be regarded as ill-conditioned. In such cases, one parameter may be fixed, reparameterised, or constrained by additional experimental information [18].

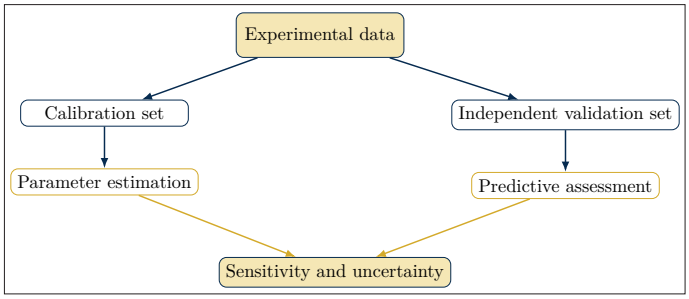


Figure 2: Separation of Experimental Information into Calibration and Independent Validation Streams, Followed by Sensitivity and Uncertainty Assessment

Objective Function and Estimation

For observations $y_j^{\exp}$ and predictions $y_j^{\mathrm{mod}}(\mathbf{p})$, a weighted objective function may be defined as

$$J(\mathbf{p}) = \sum_{j=1}^{m} w_j \left[y_j^{\mathrm{mod}}(\mathbf{p}) - y_j^{\exp} \right]^2 ,$$

where w_j reflects measurement scale, precision, or variance. When several observables are used, such as surface temperature and regression rate, normalisation should prevent the numerically larger quantity from artificially dominating the fit.

Optimisation will be initiated using robust methods and multiple starting points. The resulting solution must satisfy physical bounds. Where appropriate, a probabilistic formulation may complement deterministic estimation, allowing prior information to be combined with observed data [17,22].

Practical Identifiability

Identifiability will be examined through objective-function profiles, the sensitivity matrix, correlations, and parameter variation under perturbations of the data. A parameter is operationally useful when changes in its magnitude produce an observable signature greater than the experimental noise and cannot be almost exactly compensated by other parameters.

Excessively wide intervals or near-degenerate correlations will be reported as scientific results rather than concealed behind a single optimum value. The aim is to distinguish what the data permit one to conclude from what remains undetermined.

Sensitivity Analysis

The analysis will begin with local sensitivities around the calibrated parameter set, using normalised derivatives or controlled finite differences. Global analysis over the physically admissible range will then be performed for the most influential parameters. Global methods are particularly useful in the presence of nonlinearities, interactions, or regime-dependent effects [18].

Quantities of interest will include maximum surface temperature, response delay, mean and maximum regression rate, interface position, and energy residual. The ranking of influence may vary between regimes; sensitivity will therefore be assessed under more than one experimental condition.

Experimental Validation

Validation will be performed exclusively with data not used in the principal calibration. For each test, time series, peak values, characteristic times, and internal profiles, where available, will be compared. Residuals and normalised metrics will be calculated, but no single metric will be regarded as sufficient to validate every aspect of the response [12].

Agreement should be interpreted in the light of experimental and numerical uncertainty. A systematic deviation with persistent sign may indicate structural deficiency, whereas random scatter compatible with uncertainty may not justify increased model complexity.

Comparison Metrics

Depending on the observable, the mean error, root-mean-square error, normalised relative error, and error in integral quantities will be considered. For a series of m observations, the RMSE is

$$\mathrm{RMSE} = \sqrt{\frac{1}{m}\sum_{j=1}^{m}\left(y_j^{\mathrm{mod}} - y_j^{\mathrm{exp}}\right)^2}.$$

The metrics will be accompanied by residual plots over time and comparison with the scale of experimental uncertainty.

Numerical Example in Python – RMSE and Residuals

For demonstration only, consider five normalised measurements of regression rate and the corresponding model predictions. The following example calculates the RMSE, mean error, and residuals and can be adapted directly to the experimental data used in Phase V.

```
import numpy as np

y_exp = np.array([0.82, 0.95, 1.10, 1.18, 1.31])
y_mod = np.array([0.80, 0.98, 1.07, 1.21, 1.28])

res = y_mod - y_exp
rmse = np.sqrt(np.mean(res**2))
bias = np.mean(res)
rel = 100*rmse/np.mean(y_exp)

print(f"RMSE = {rmse:.4f}")
print(f"Mean error = {bias:.4f}")
print(f"Relative RMSE = {rel:.2f}%")
print("Residuals =", res)

import matplotlib.pyplot as plt
j = np.arange(1, len(y_exp)+1)
plt.plot(j, y_exp, 'o-', label='Experiment')
plt.plot(j, y_mod, 's--', label='Model')
plt.xlabel('Observation')
plt.ylabel('Normalised regression rate')
plt.title('Model--experiment comparison')
plt.grid(True)
plt.legend()
plt.show()
```

For this illustrative dataset, the RMSE is approximately 0.0277, the relative RMSE is about 2.57%, and the mean error is −0.004, which is small compared with the response scale. The complementary metrics distinguish overall discrepancy from systematic bias; actual validation must additionally compare these values with experimental uncertainty.

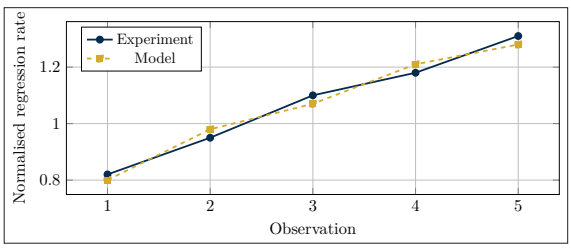


Figure 3: Approximate Model–Experiment Comparison for the Python Validation Example. The Predictions Follow the Measured Trend with small Alternating Discrepancies

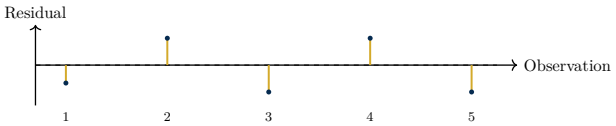


Figure 4: Illustrative Residual Pattern for the Normalised Regression-Rate Example; Residuals are Model Predictions Minus Experimental Observations

Uncertainty Quantification and Propagation

Sources of uncertainty will be organised into four classes: measurement, parameters, initial/ boundary conditions, and numerical approximation. Where justified probability distributions are available, uncertainties will be propagated by sampling. Where only defensible intervals are available, results will be presented as envelopes or scenario analyses, avoiding artificial probability distributions unsupported by empirical evidence [22].

The principal output will be expressed as a central prediction accompanied by an uncertainty interval or band. Its width should be interpreted together with sensitivity: reducing uncertainty in a weakly influential parameter has limited value, whereas improving the measurement of a dominant parameter may substantially reduce predictive uncertainty.

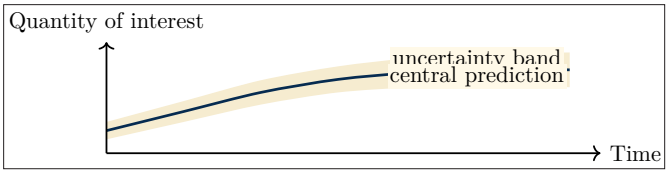


Figure 5: Schematic Propagation of Input Uncertainty to a Time-Dependent Quantity of Interest. The Coloured Band Represents Predictive Uncertainty Around the Central Model Response

Model Discrepancy

Even with optimised parameters, the model may exhibit structural discrepancy due to omitted mechanisms, geometric simplifications, or incomplete constitutive laws. Such discrepancy should not be indiscriminately absorbed by calibrated parameters. Comparison across regimes and observables will help identify error patterns and determine whether a subsequent version requires temperature-dependent properties, multiple kinetics, radiation, or more detailed gas-phase coupling [25].

Acceptance Criteria for Phase V

The phase will be regarded as complete when: the separation between calibration and validation data is documented; fitted parameters are physically admissible; identifiability has been assessed; the numerical solution used in calibration has controlled discretisation error; predictions have been compared with independent data; and uncertainty in the principal quantities of interest has been quantified.

No universal error threshold unrelated to the application will be adopted. Quantitative criteria should be defined according to experimental accuracy, the intended purpose of the model, and the magnitude of the quantities being assessed.

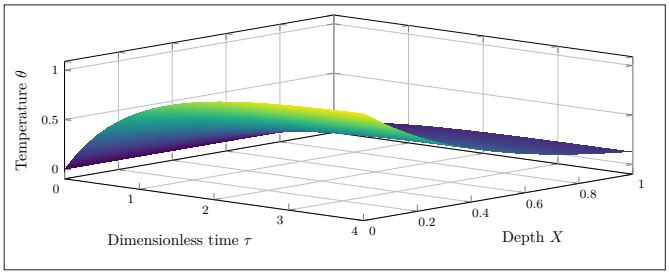


Figure 6: Illustrative Dimensionless Temperature Surface Showing Transient Thermal Penetration from the Regressing Interface into the Solid. The Surface is Schematic and is Intended to Visualise the Model Structure Rather than Experimental Data

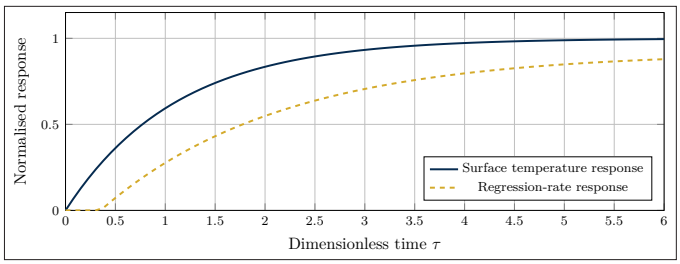


Figure 7: Responses Associated with Thermal Memory. The Curves Emphasise the Different Relaxation Scales of Surface Temperature and Regression Rate

Phase V Implementation Plan

1. inventory and qualify the available experimental data;
2. separate calibration and validation datasets in advance;
3. define free parameters, bounds, and independent information;
4. perform preliminary sensitivity and identifiability analyses;
5. calibrate from multiple starting points and record convergence;
6. validate against independent tests and analyse residuals;
7. propagate uncertainties to the quantities of interest;
8. document limitations, the application domain,and requirements for new experiments.

Phase V Deliverables
D1. Qualified and separated experimental database. **D2**. Calibrated parameters with uncertainty intervals. **D3**. Identifiability and sensitivity report. **D4**. Validation against independent data. **D5**. Predictive uncertainty bands. **D6**. Recommendations for model extension and new experiments.

Conclusion of Phase V

Phase V completes the first full cycle of the project, from physical specification to quantitative assessment against data. The model ceases to be merely a mathematically coherent and numerically verifiable construction and becomes a scientific hypothesis tested against independent observations. Separating calibration from validation safeguards interpretation and reduces the risk of confusing goodness of fit with predictive capability.

Identifiability analysis adds an essential dimension. Not every parameter appearing in an equation can be estimated from the available data, and not every optimum value is physically informative. By examining sensitivities, correlations, and fitting profiles, Phase V determines which mechanisms are effectively observable and which require new measurements or model simplification.

Uncertainty quantification transforms a point prediction into a prediction accompanied by a measure of confidence. Experimental, parametric, numerical, and structural uncertainties have different origins and should be distinguished. This decomposition identifies where experimental or computational investment is most likely to reduce final predictive uncertainty. Validation also serves as a structural diagnostic. Systematic residuals, incorrect delays, or regime-dependent errors may reveal missing mechanisms. Rather than increasing complexity automatically, the project requires every extension to respond to an identified discrepancy and to be supported by data capable of constraining the new parameters.

This phase establishes the conditions for broader parametric studies, comparison among constitutive formulations, and eventual extension to more complex geometries or mechanisms. Further development should preserve the same methodological discipline: explicit hypotheses, traceable formulation, numerical verification, independent validation, and transparent communication of uncertainty.

General Conclusion

The work developed throughout Phases I–V constitutes an integrated framework for studying the unsteady combustion of a solid propellant. The sequence was deliberately progressive: the physics was defined, the dimensional equations formulated, dimensionless scales constructed, a verifiable numerical method established, and finally a protocol for calibration, validation, and uncertainty quantification specified. This ordering makes it possible to trace each result back to the assumptions from which it originated.

In Phase I, heat conduction, decomposition, surface regression, and heat feedback from the gas phase were selected as the fundamental mechanisms. Phase II translated this specification into a dimensional system and treated the moving boundary through a coordinate transformation that preserves interface kinematics. Dimensional verification and limiting cases provide essential safeguards against formulation errors [4].

Phase III showed that normalisation by physical scales makes the competition among regression, kinetics, heat transfer, and interfacial energy more transparent. The resulting dimensionless groups facilitate regime comparison and guide both experimental design and the selection of numerical parameters.

In Phase IV, the combination of finite differences, implicit time integration, transport treatment, and nonlinear iteration was accompanied by progressive tests, mesh refinement, and energy-balance control. Numerical verification is a scientific requirement: before comparison with experiments, it must be demonstrated that the implementation solves the governing equations with controlled discretisation error [11,12].

Phase V introduced systematic confrontation with independent data. Separating calibration from validation prevents the same information from being used both to fit and to substantiate the model. Identifiability, sensitivity, and uncertainty quantification show not only which prediction is obtained, but also which parameters control it and with what confidence it may be used [17,18,22].

The project therefore adopts a concept of quality based on distinct forms of evidence: physical coherence, dimensional consistency, numerical convergence, and experimental agreement. A model may

fit calibration data yet fail validation; it may contain appropriate physics but be compromised by inadequate discretisation; or it may require new mechanisms when residuals reveal systematic discrepancies. The phased structure is designed to distinguish among these situations.

Future complexity should increase in a controlled manner. Temperature-dependent properties, radiation, multiple kinetics, porosity, or more detailed gas-phase coupling should be introduced only when evidence demonstrates the insufficiency of the preceding version and when data exist to constrain the additional parameters. Initial conditions, parameters, meshes, tolerances, code versions, and data-processing procedures should remain recorded to ensure reproducibility [35-43].

In summary, the five phases provide a coherent basis for predictive research on unsteady combustion with a moving boundary and thermal memory. The value of the model lies in the transparency with which it relates mechanisms, equations, computational solution, data, and uncertainties. Subsequent work may explore the parameter space and deepen the physics while preserving the traceability, verification, and validation criteria established in this document.

Final Synthesis
The project now provides a complete chain: **physical foundations → dimensional formulation → dimensionless analysis → numerical verification → calibration and experimental validation**. This chain forms the basis for predictive research, model extension, and scientific publication.

Final Declarations

Conflict of Interest. The authors declare that there is no conflict of interest associated with this work.

CRediT Author Statement. Conceptualisation, methodology, physico-mathematical formulation, analysis, validation, writing, and review: Manuel J. Alves and Elena V. Alves.

Funding. No specific funding was reported for the preparation of this project.

Declaration on the Use of Artificial Intelligence. Artificial-intelligence tools were used solely to assist the translation of the original Portuguese text, written in accordance with AO90, into British Academic English and to support linguistic revision. The scientific content, mathematical formulation, equations, interpretation of results, references, and final scholarly responsibility remain entirely with the authors, who reviewed and approved the final text.

Reference

1. Williams FA (1985) Combustion Theory. 2nd ed., Benjamin/Cummings.
2. Law CK (2006) Combustion Physics. Cambridge University Press.
3. Sutton GP, Biblarz O (2017) Rocket Propulsion Elements. 9th ed., Wiley.
4. Crank J (1984) Free and Moving Boundary Problems. Clarendon Press, Oxford.
5. Barenblatt GI (1996) Scaling, Self-Similarity, and Intermediate Asymptotics. Cambridge University Press.
6. Buckingham E (1914) On physically similar systems; illustrations of the use of dimensional equations. Physical Review 4: 345-376.
7. Patankar SV (1980) Numerical Heat Transfer and Fluid Flow. Hemisphere.
8. Ferziger JH, Perić M (2020) Street, R. L. Computational Methods for Fluid Dynamics. 4th ed., Springer.
9. Thomas JW (1995) Numerical Partial Differential Equations: Finite Difference Methods. Springer.
10. Versteeg HK, Malalasekera W (2007) An Introduction to Computational Fluid Dynamics: The Finite Volume Method. 2nd ed., Pearson.
11. Roache PJ (1998) Verification and Validation in Computational Science and Engineering. Hermosa Publishers.
12. Oberkampf WL, Roy CJ (2010) Verification and Validation in Scientific Computing. Cambridge University Press 2010
13. (2009) ASME V&V 20–2009: Standard for Verification and Validation in Computational Fluid Dynamics and Heat Transfer. ASME.
14. Helton JC, Davis FJ (2003) Latin hypercube sampling and the propagation of uncertainty in analyses of complex systems. Reliability Engineering & System Safety 81: 23-69.
15. Homma T, Saltelli A (1996) Importance measures in global sensitivity analysis of nonlinear models. Reliability Engineering & System Safety 52: 1-17.
16. Sobol, IM (2001) Global sensitivity indices for nonlinear mathematical models and their Monte Carlo estimates. Mathematics and Computers in Simulation 55: 271-280.
17. Kennedy MC, OHagan A (2001) Bayesian calibration of computer models. Journal of the Royal Statistical Society: Series B 63: 425-464.
18. Saltelli A, Marco Ratto, Terry Andres, Francesca (2008) Global Sensitivity Analysis: The Primer. Wiley DOI:10.1002/9780470725184.
19. Turns SR (2012) An Introduction to Combustion: Concepts and Applications. 3rd ed., McGraw-Hill.
20. Bergman TL, Lavine AS, Incropera FP, DeWitt DP (2011) Fundamentals of Heat and Mass Transfer. 7th ed., Wiley.
21. Kuo KK, Acharya R (2012) Fundamentals of Turbulent and Multiphase Combustion. Wiley.
22. Smith RC (2014) Uncertainty Quantification: Theory, Implementation, and Applications. SIAM.
23. Zeldovich Y B, Barenblatt GI, Librovich VB, Makhviladze GM (1985) The Mathematical Theory of Combustion and Explosions. Consultants Bureau.
24. Glassman I, Yetter RA, Glumac NG (2014) Combustion. 5th ed., Academic Press.
25. Barrère M, Jaumotte A, Veubeke BF, Vandenkerckhove J (1960) Rocket Propulsion. Elsevier.
26. Kuo KK (1986) Principles of Combustion. Wiley.
27. Beckstead MW, Derr RL, Price CF (1970) A model of composite solid-propellant combustion based on multiple flames. AIAA Journal 8: 2200-2207.
28. Coleman HW, Steele WG (2009) Experimentation, Validation, and Uncertainty Analysis for Engineers. 3rd ed., Wiley.
29. Landau LD, Lifshitz EM (1987) Fluid Mechanics. 2nd ed., Pergamon Press.
30. Frank-Kamenetskii DA (1969) Diffusion and Heat Transfer in Chemical Kinetics. 2nd ed., Plenum Press.
31. Friedman A (1964) Partial Differential Equations of Parabolic Type. Prentice-Hall.
32. Bird RB, Stewart WE, Lightfoot EN (2002) Transport Phenomena. 2nd ed., Wiley.
33. Çengel YA, Ghajar AJ (2020) Heat and Mass Transfer: Fundamentals and Applications. 6th ed., McGraw-Hill.
34. LeVeque RJ (2007) Finite Difference Methods for Ordinary and Partial Differential Equations. SIAM.
35. Alves EV, Yevgrashin YB, Molchanov VF (2019) Analytical solution of the equation of a burning surface. Far East Journal

of Applied Mathematics 102: 31-37.

36. Alves EV, Alves MJ (2018) Equation for calculating the burning rate for solid propellants. Far East Journal of Applied Mathematics 100: 153-165.
37. Alves EV, Alves MJ (2018) Fundamental solution of heat equation in condensed phase. Far East Journal of Applied Mathematics 100: 167-180.
38. Alves EV, AlvesMJ (2018) Linearized integral equation for burning rate of solid propellants. Far East Journal of Applied Mathematics 100: 217-233.
39. Alves EV, Molchanov VF, Tagilova EA (2013) Flow of non-Newtonian fluid between parallel planes. Far East Journal of Applied Mathematics 78: 67-73.
40. Alves EV, Molchanov VF, Tagilova EA (2017) Flow of non-Newtonian fluid between coaxial cylindrical surfaces. Far East Journal of Applied Mathematics 95: 401-409.
41. Alves M, Alves E, Leão A (2018) On the boundary-value problem for a singular differential equation. Far East Journal of Applied Mathematics 100: 139-152.
42. Alves E, Alves M, Labovskiy S (2022) On periodic spectral problem for a functional-differential equation of even order. Far East Journal of Applied Mathematics 115: 61-68.
43. Moin P (2010) Fundamentals of Engineering Numerical Analysis. 2nd ed., Cambridge University Press.

Copyright: ©2026 Elena Vladimirovna Alves and Manuel Joaquim Alves. This is an open-access article distributed under the terms of the Creative Commons Attribution License, which permits unrestricted use, distribution, and reproduction in any medium, provided the original author and source are